Estimation of Phase Errors in SAR Data by Local-Quadratic Map-Drift Autofocus

Oleksandr O. Bezvesilniy, Ievgen M. Gorovyi, and Dmytro M. Vavriv
Department of Microwave Electronics, Institute of Radio Astronomy of NAS of Ukraine
4 Chervonopraporna Str., Kharkov 61002, Ukraine
obezv@rian.kharkov.ua, gorovoy@rian.kharkov.ua, vavriv@rian.kharkov.ua

Abstract— **Uncompensated phase errors lead to quality degradation of SAR images what is especially critical for high-resolution systems. In the paper, a novel approach to the stripmap autofocus is proposed. The idea of the method is to estimate the local quadratic phase errors by processing small data blocks. The conventional map-drift autofocus (MDA) algorithm is used for such estimation. Then, by a double integration of the estimated quadratic errors, an arbitrary residual phase error for large data blocks is evaluated. The performance of the proposed method is demonstrated with data obtained with an X-band airborne SAR system.**

Keywords— synthetic aperture radar; motion errors; autofocus; map-drift; motion compensation

I. INTRODUCTION

The quality of synthetic aperture radar (SAR) images essentially depends on the precision of trajectory measurements of the SAR platform [1]-[3]. Provided the aircraft trajectory is measured carefully, the conventional methods of the motion compensation [2] can be used to produce high quality SAR images. However, the requirements to the accuracy of trajectory measurements in modern SAR systems are often very high, as well as the cost of the navigation systems, which could provide the required precise measurements. To solve the problem, a number of methods for the estimation of motion errors directly from the received radar data have been developed so far [1]-[4]. These methods are known as autofocus methods.

The phase errors in the received data can be measured directly from the phase of signals backscattered by bright point targets. This is realized in the well-known prominent point processing (PPP) method [3]. Another effective technique is the phase gradient autofocus (PGA) [3], [5]-[7], which estimates the first derivative (gradient) of the phase error from signals of isolated point scatterers. These two methods are advantageous over other methods since they do not use any model of the phase errors, and, therefore, they can be used to estimate an arbitrary phase error function.

However, the PPP and PGA methods are intended for the spotlight SAR mode. In this mode, the antenna is controlled to illuminate a selected spot on the ground. As the result, the signal from each illuminated target is presented in every received radar pulse. It means that the signal of each point scatterer on the scene contains the motion error function for the whole time of the data acquisition. In the spotlight mode, the PPP and PGA methods work quite well.

In the strip-map mode, the situation is more complicated. The antenna illuminates a strip aside of the aircraft flight path, and point targets echoes are presented in the received data only during the time required for a target to cross the antenna beam. It means that the phase errors estimated from the signals of several selected point targets represent only small parts of the complete phase error function, which should be determined for the whole time of a large data frame. Thus, in the strip-map mode, we face the problem of "stitching" the phase errors estimated on short time intervals into the complete error function on a long time interval.

For the stripmap mode, the autofocus methods, which are based on signals from point targets, require many scatterers to be presented on the scene. Therefore, it is better to use autofocus methods, which required only the presence of contrast features on the scene, such as edges, shadows, and other details but not necessarily the bright points. The map-drift autofocus (MDA) [3], [8]-[12] is a good example of such method.

The map-drift autofocus (MDA) is used to estimate the quadratic phase error (the mismatch between the received signal and the SAR reference function) by measuring a linear shift between two SAR images built by dividing the processing interval in the azimuth on two parts. The multiple-aperture map-drift autofocus [3], [13] can estimate a more general phase error modeled by a polynomial by measuring the relative shifts in a sequence of more than two SAR images. It should be mentioned here that the application of a model for the complete phase error function on the long time interval helps to combine local estimates into the long error function. Other models such as Fourier series have also been proposed [13]-[15] to approximate an arbitrary phase error function.

In this paper, we propose a novel approach to the stripmap SAR autofocus. We name it as Local-Quadratic Map-Drift Autofocus (LQMDA). The idea of the method is to estimate the local quadratic phase errors on small time intervals. These estimates represent the second derivative of an arbitrary phase error function. The error function is evaluated then by a double integration avoiding the "stitching problem" and without introducing any models for the complete phase error function. The proposed LQMDA has several similarities with the reflectivity displacement method (RDM) [16]-[18]. Both

978-1-4577-1837-3/12/$26.00

methods use local estimates of the motion errors and the integration step to evaluate the complete phase error function. However, we believe that the proposed LQMDA is more accurate since it does not use the simplifying assumptions of the RDM approach.

In Sections II, the principle of the representation of an arbitrary phase error function by local quadratic phase errors is described. The estimation of the local quadratic errors by using the MDA on short intervals is considered in Section III. Section IV provides block-schemes for the implementation of the proposed LQMDA on practice. In Section V, the effectiveness of the approach is illustrated by using data obtained with an X-band airborne SAR system [19] operated from a light-weight aircraft.

II. Representation of an Arbitrary Phase Error Function by Local Quadratic Phase Errors

Many of the strip-map mode SAR processing algorithms, like the well-known range-Doppler algorithm (RDA) [4], perform processing of the received data by large data blocks (frames). The size of the block in the azimuth direction includes usually many intervals of the synthesis. These algorithms are rather efficient due to the application of the fast Fourier transform (FFT) for the synthesis. Such processing implies that a SAR platform moves along a straight line with a constant velocity and a stable antenna orientation during the whole data acquisition time of the frame. However, in real conditions, the actual aircraft trajectory deviates from the expected reference flight line. These deviations if not compensated lead to a degradation of SAR image quality.

If the actual flight trajectory is measured accurately by the SAR navigation system, the motion errors in the received data can be compensated by using motion compensation procedures [2] that perform:

1) the correction of the range migration errors, $\Delta R_E(R,t)$,

2) the compensation of the corresponding phase errors, $(4\pi/\lambda)\Delta R_E(R,t)$.

The errors depend on the slant range R and the azimuth ("slow") time t; λ is the radar wavelength.

The problem is that the accuracy of the SAR navigation system may be insufficient to achieve a required SAR resolution. As the result, unknown residual phase errors are still presented in the data after the motion error compensation.

Let $s(R,t)$ be the SAR data after the range compression and the range cell migration correction. We also assume that the motion error compensation based on the measured trajectory has been applied. The data are ready for the azimuth compression but they contain the residual phase errors $\varphi_E(R,t)$:

$$s(R,t) = s_{ref}(R,t)\exp[i\varphi_E(R,t)].$$

Here $s_{ref}(R,t)$ is the signal expected for the reference flight conditions. From now, we shall consider the problem for a given range R and simplify the notation to $\varphi_E(t)$, $s(t)$, etc.

Let us divide the whole data frame $0 \le t \le T_{FR}$ of the duration T_{FR} on short half-overlapped intervals of the duration T_S with the centers at the moments of time

$$t_n = (2n+1)(T_S/2),\ n = 0, 1, ..., N.$$

We shall assume that these intervals are short enough so that the residual phase error within each interval can be approximated by the 2-nd order polynomial:

$$\varphi_E(t_n+\tau) \approx \varphi_E(t_n) + \varphi'_E(t_n)\tau + \varphi''_E(t_n)\tau^2/2, \qquad (1)$$

τ is the time within the short interval $-T_S/2 < \tau < T_S/2$.

We propose to estimate the local quadratic errors on each short internal separately by using the map-drift autofocus (MDA). According to this autofocus technique, the short processing interval is divided on two parts, and two SAR images are built. If there is no quadratic error on the short interval, the two images will coincide. The presence of the quadratic error shifts the images in the azimuth in the opposite directions. By measuring this shift the local quadratic error term $\varphi''_E(t_n)\tau^2/2$ can be estimated. The constant term $\varphi_E(t_n)$ does not affect the estimation and can be omitted, as well as the linear term $\varphi'_E(t_n)\tau$ which only shifts the two SAR images in the azimuth in the same direction.

As the result of such processing, we can estimate the samples of the second derivative of the residual error function as illustrated in Fig. 1. By a double integration, we can evaluate the unknown residual error function for the whole data frame, and use it for the phase compensation.

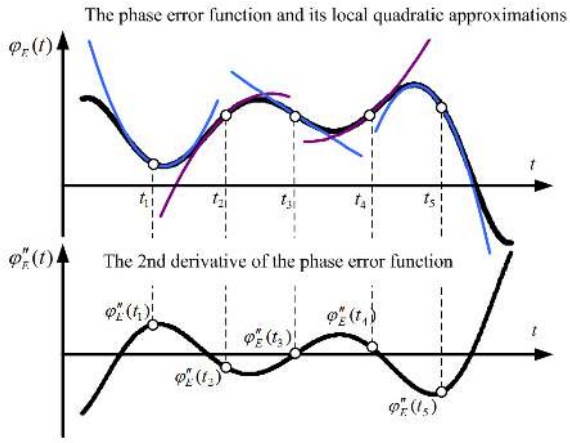

Figure 1. The unknown residual phase error function, its quadratic approximations, and the 2-nd derivative of the error function to be estimated.

During the integration, the problems of the unknown integration constants and noise-induced trends arise. We solve these problems by using the trajectory measured by the SAR navigation system as the reference, assuming that the residual phase errors should not demonstrate any trends on the large interval of the whole data frame.

III. MDA PROCESSING ON A SHORT INTERVAL

In this section, we consider the MDA processing on a short interval with the convolution-based SAR processing algorithm.

A. Peculiarities of SAR Data Processing on a Short Interval

The SAR image built by processing the data collected on a short time interval shows a part of the ground scene that was illuminated by a real antenna beam during this short flight time. Modern SAR systems are usually equipped with rather wide-beam antennas in the azimuth direction to realize multi-look SAR processing for the speckle noise suppression [1]-[4]. Therefore, the area illuminated during the short interval represents approximately the area of the antenna footprint as illustrated in Fig. 2. In the figure, one can see the antenna footprints on the ground plane for three positions of the aircraft: 1) at the beginning, 2) at the center, and 3) at the end of the short interval.

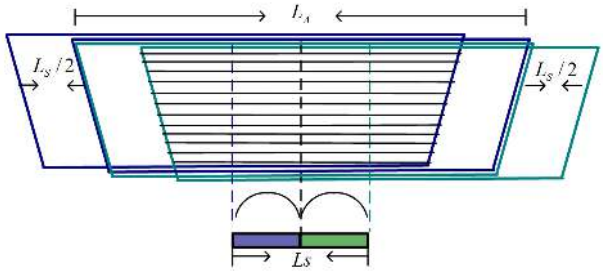

Figure 2. Radar data in the time domain and the antenna footprints.

For instance, for the antenna beam width $\theta_A = 10°$ in the azimuth, the antenna footprint on the ground at the slant range $R = 4$ km is approximately $L_A \approx R\theta_A \approx 700$ m. The synthetic aperture length required to achieve the azimuth resolution $\rho = 3$ m is only $L_S \approx K_w \lambda R/(2\rho) \approx 26$ m ($\lambda = 3$ cm and the weighting window coefficient $K_w = 1.3$).

Thus, the SAR images, which are built from the short half-intervals for the MDA estimation, will represent two highly overlapped antenna footprints. The shift between such images can be easily measured and used to estimate the local quadratic errors.

The Doppler bandwidth of the SAR data collected on a short interval is limited by the antenna beam width:

$$\Delta F_A \approx (2/\lambda) V \theta_A , \qquad (2)$$

V is the aircraft flight velocity. However, the Doppler bandwidth of the signal of any point target is much smaller:

$$\Delta F_\rho = K_w V / \rho . \qquad (3)$$

This bandwidth covers only a small part of the whole spectrum as shown in Fig. 3. The central frequency F_T of the target spectrum corresponds to the position of the target within the footprint.

Thus, the azimuth sampling frequency of the received data should be high enough to represent the wide data bandwidth ΔF_A (2). At the same time, the data are significantly oversampled as compared to the bandwidth ΔF_ρ (3), required to achieve the desired resolution.

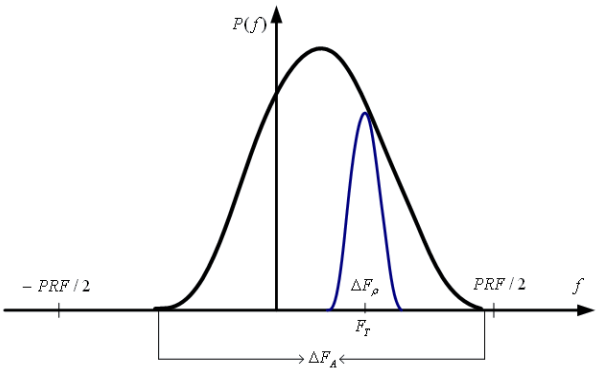

Figure 3. Radar data on the short interval in the Doppler domain.

B. SAR Processing via Convolution in Time Domain or in Frequency Domain

We introduce right and left SAR images for the MDA via the convolution in the time domain as follows:

$$I_L(t) = \frac{2}{T_S} \int_{-T_S/2}^{0} w_S(\tau + T_S/4) s(\tau) h^*(\tau - t) d\tau , \qquad (4)$$

$$I_R(t) = \frac{2}{T_S} \int_{0}^{T_S/2} w_S(\tau - T_S/4) s(\tau) h^*(\tau - t) d\tau , \qquad (5)$$

$$-T_A/2 \le t \le T_A/2 , \quad T_A \approx R\theta_A / V .$$

The weighting window $w_S(\tau)$ of the length of $T_S/2$ is applied in the time domain to each of the half-intervals separately.

The reference function $h(t)$ is defined on the whole length of the antenna footprint $-T_A/2 \le t \le T_A/2$ as

$$h(t) = w_H(t) \exp[2\pi i (F_{DC} t + F_{DR} t^2/2)] , \qquad (6)$$

where F_{DC} and F_{DR} are the Doppler centroid and Doppler rate. The weighting window $w_H(t)$ of the reference function of the length T_A is introduced to limit the processed Doppler bandwidth to the Doppler bandwidth ΔF_A (2) determined by the antenna beam width.

The described map-drift autofocus can be called "local map-drift autofocus". In this approach, the data are divided in two parts, and we estimate local quadratic error in the data. It is different from the classical map-drift autofocus [8]-[11], in which the reference function is divided in two parts, and the quadratic error to be estimated is the error in the reference function.

Alternatively, the convolutions (4)-(5) can be calculated via the Doppler frequency domain (by using FFT):

$$I_{L,R}(t) = \int_{-\Delta F_A/2}^{\Delta F_A/2} S_{L,R}(f) H^*(f) \exp[2\pi i f t] df ,$$

$$S_L(f) = \frac{2}{T_S} \int_{-T_S/2}^{0} w_S(\tau + T_S/4) s(\tau) \exp[-2\pi i f \tau] d\tau ,$$

$$S_R(f) = \frac{2}{T_S} \int_{0}^{T_S/2} w_S(\tau - T_S/4) s(\tau) \exp[-2\pi i f \tau] d\tau ,$$

$$H(f) = \int_{-T_A/2}^{T_A/2} w_H(t) h(t) \exp[-2\pi i f t] dt .$$

Processing on a short interval in the Doppler domain has several differences as compared to the conventional RDA processing applied to the large data frame that includes many intervals of the synthesis. First, in the conventional RDA, the reference function is built for the short Doppler bandwidth (3) determined by the required resolution. While processing the data on the short interval, which represents only one synthetic aperture, we should build the reference function for the whole Doppler bandwidth (2) to obtain the image of the antenna footprint. Second, the window $w_H(t)$ applied to the long reference function in the time domain (and the corresponding window in the Doppler frequency domain) does not weight the short spectra of individual point targets, as it is evidently seen from Fig. 3. Therefore, the data on the short half-intervals should be multiplied by the window $w_S(\tau)$ in the time domain before transformation into the frequency domain. In this way, the individual target spectra will be weighted properly.

Let us derive the main formula of the map-drift autofocus that relates the shift between the left and right images to the local quadratic error. The signal of unit amplitude from a point target distorted by the quadratic error (1) on the short interval can be written as follows:

$$s(\tau) = w_A(\tau - t_p) \exp[2\pi i (F_{DR}(\tau - t_p)^2/2 + \Delta F_{DR}^E \tau^2/2)] , \quad (7)$$

$$\Delta F_{DR}^E = \varphi_E''(t_n)/(2\pi) . \quad (8)$$

We omit in (7) the linear phase term caused by the Doppler centroid and the linear term of the local phase errors (1), since they just shift both the left and right images in the same way. The window $w_A(t)$ in (7) describes the real antenna beam pattern. The moment of time t_p indicates the azimuth position of the target: at that moment the target crosses the center of the antenna beam at the slant range R. The local quadratic phase error (8) has to be estimated by the MDA.

The relation between the shift and the quadratic error can be derived by substituting the signal (7) and the reference function (6) into the time-domain formulas (4)-(5). For simplicity, we ignore the antenna window $w_A(t)$ and use rectangular windows for $w_S(t)$ and $w_H(t)$. Also, we disregard the defocusing effect caused by the quadratic phase error term $\exp[\pi i \Delta F_{DR}^E \tau^2]$ on the short half-intervals (to obtain sinc-functions instead of Fresnel integrals). Under such assumptions, one can derive the following formulas for the left and right SAR images of a point target:

$$|I_L(t)| \approx |\mathrm{sinc}[\pi \{F_{DR}(t - t_p) - \Delta F_{DR}^E (T_S/4)\}(T_S/2)]| ,$$

$$|I_R(t)| \approx |\mathrm{sinc}[\pi \{F_{DR}(t - t_p) + \Delta F_{DR}^E (T_S/4)\}(T_S/2)]| .$$

The point target in the images is shifted from its true position $t = t_p$ in the opposite directions to new positions determined by the maxima $t_{R,L\max}$ of the sinc-functions. The relative shift depends on the local quadratic phase error:

$$\Delta t_{\max} = t_{R\max} - t_{L\max} = \frac{\Delta F_{DR}^E (T_S/2)}{F_{DR}} .$$

This shift is usually measured as the position of the maximum of the correlation function:

$$R(\Delta t) = \int |I_L(t)|^2 |I_R(t + \Delta t)|^2 \, dt .$$

In practice, in order to improve the peak of the correlation function, we calculate the correlation of the SAR images represented in the logarithmic scale (in decibels). We also apply local centering and normalization procedures. Such processing emphasizes variations of the scene, enhances edges and contrast features, reduces the undesirable influence of very bright targets, increases the contribution of shadows and other contrast and not very bright image features in the correlation peak.

As it has been mentioned, the azimuth sampling frequency of the data should be sufficient to represent the wide Doppler bandwidth ΔF_A (2) and unambiguously sample the long reference function (6). It means that both the time-domain and frequency domain convolution-based approaches require a lot of computations. In future, we are planning to try the well-known dechirp processing technique [3]-[4] as an alternative method to be used instead of the convolution-based approach.

IV. Incorporation of the LQMDA into the Conventional Range-Doppler Algorithm

The LQMDA can be easily incorporated into the conventional SAR processing algorithm such as the RDA, as illustrated in Fig. 4. At first, the received raw data are compressed in range and the 1st-order (range-independent) motion compensation is applied. Then, the range cell migration correction (RCMC) is performed in the range-Doppler domain. After that, the 2nd-order (range-dependent) motion compensation is accomplished. The motion compensation is based on the flight trajectory measured by the SAR navigation system. After these steps, the data is ready for the application of the LQMDA, which is intended to estimate and compensate the residual phase errors.

The main stages of the LQMDA algorithm are shown in Fig. 5. The whole data frame is divided on short data blocks in the azimuth direction. Each data block is split on two halves

and two SAR images (left and right) are synthesized. Then, the local quadratic phase errors are estimated for each data block via the map-drift autofocus. After that, by the double integration, the phase error function is calculated for the whole processed data frame. The phase compensation is applied to the data to correct the residual phase errors.

After the LQMDA, the data is ready for the conventional RDA synthesis of the corrected large data frame in the range-Doppler domain (see Fig. 4), producing the well-focused SAR image.

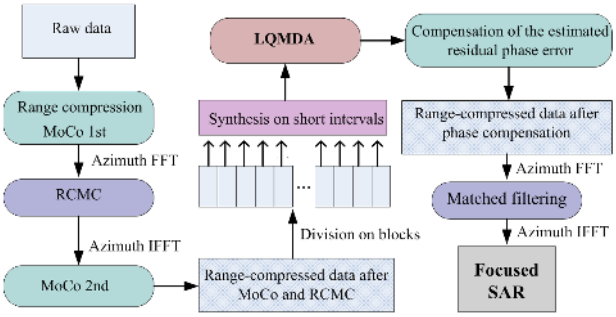

Figure 4. Incorporation of the LQMDA into the SAR processing algorithm.

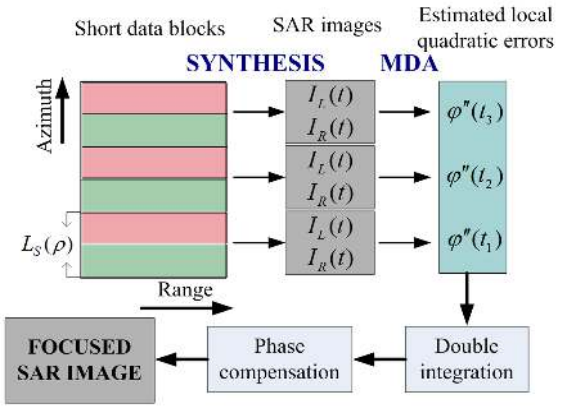

Figure 5. The block-scheme of the LQMDA algorithm.

As one can note, throughout the paper we have considered the autofocusing problem for a signal from a particular slant range. To improve the accuracy of the estimation of the complete phase error function, it is very useful to average the functions estimated on adjacent range gates. However, actually, the phase errors essentially depend on range, especially for low-altitude, wide-swath or squint-mode strip-map SARs. In the near future, we are planning to account for this range-dependence of the residual phase errors in the similar way as it was done in our multi-look contrast optimization autofocus [20]. Namely, the range dependence can be naturally incorporated in the autofocus algorithm, if we turn our consideration from the estimation of the local quadratic phase errors to the uncompensated local accelerations, or, in other words, from the residual phase error function to the residual trajectory deviations.

V. Experimental Results

In this section, the performance of the proposed LQMDA algorithm is illustrated. The data were obtained with the airborne RIAN-SAR-X system [19] developed and produced at the Institute of Radio Astronomy of the National Academy of Sciences of Ukraine. The radar operates in the X-band. During the experiments, the radar was installed on a light-weight aircraft Antonov AN-2.

An example of the slant range error measured by the SAR navigation system based on a GPS receiver is shown in Fig. 6a. The slant range error is up to about 10 meters during the large data frame of about 30 s. The aircraft flight velocity was about 40 m/s, and the flight altitude was about 1900 m. The residual range error estimated by using the LQMDA algorithm is shown in Fig. 6b, and it demonstrates variations within ± 30 cm.

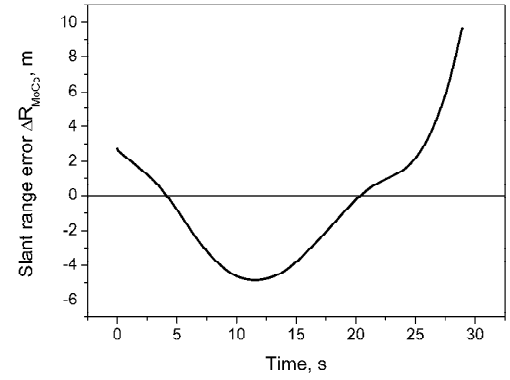

(a)

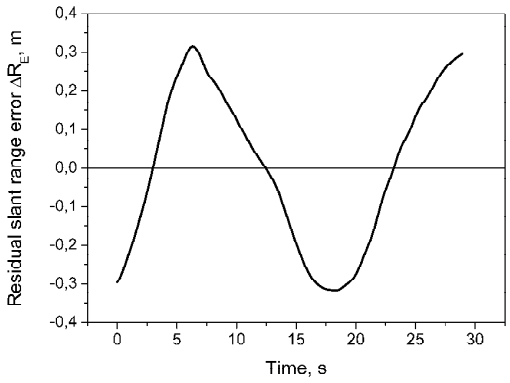

(b)

Figure 6. The slant range error measured by the SAR navigation system (a) and the residual phase error estimated by the proposed LQMDA algorithm (b).

A 25-look SAR image with 3-meter resolution built without autofocusing is shown in Fig 7a. One can see that the residual error shown in Fig. 6b results in strong defocusing of the image. The well-focused SAR image built with the proposed LQMDA algorithm is shown in Fig. 7b. The experimental results prove evidently the efficiency of the proposed autofocusing approach.

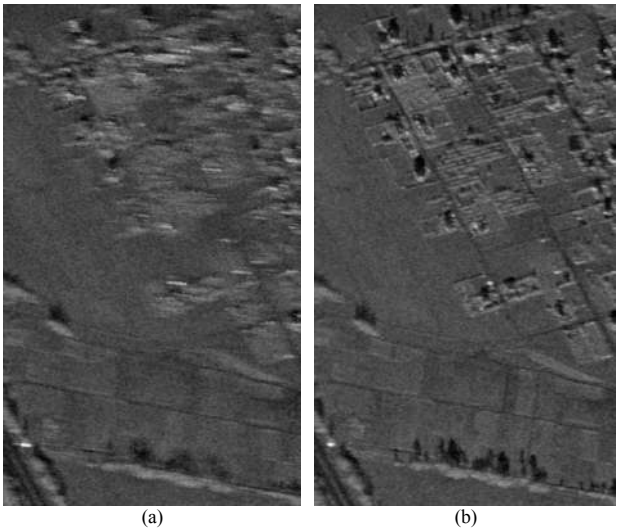

(a) (b)

Figure 7. SAR images (25 looks, 3-meter resolution) built without autofocusing (a) and with the proposed LQMDA algorithm. (b).

VI. CONCLUSION

We have developed and tested an effective autofocusing approach for stripmap SAR systems. The method can estimate arbitrary residual phase errors by the integration of the local quadratic errors found with the conventional MDA. The real data examples prove a high performance of the proposed method. Although the LQMDA algorithm was developed for the stripmap mode, it is perfectly applicable for the spotlight mode as well.

REFERENCES

[1] C. Oliver and S. Quegan, Understanding Synthetic Aperture Radar Images. Norwood, MA: Artech House, 1999.

[2] G. Franceschetti and R. Lanari, Synthetic Aperture Radar Processing. CRC Press, 1999.

[3] W. G. Carrara, R. S. Goodman, and R. M. Majewski, Spotlight Synthetic Aperture Radar: Signal Processing Algorithms. Boston; London: Artech House, 1995.

[4] I. G. Cumming and F. H. Wong, Digital Processing of Synthetic Aperture Radar Data: Algorithms and Implementation". Norwood, MA: Artech House, 2005.

[5] D. E. Wahl, P. H. Eichel, D. C. Ghiglia, and C. V. Jakowatz, Jr., "Phase gradient autofocus – A robust tool for high resolution phase correction", IEEE Trans. Aerosp. Electron. Syst., vol. 30, no. 3, pp. 827–835, 1994.

[6] D. E. Wahl, C. V. Jakowatz Jr., P. A. Thompson, and D. C. Ghiglia, "New approach to strip-map SAR autofocus". Sixth IEEE Digital Signal Processing Workshop, IEEE, pp. 53–56, 1994.

[7] M. P. Hayes, H. J. Callow, and P. T. Gough, "Stripmap phase gradient autofocus," in Proc. OCEANS, Sep. 22–26, 2003, vol. 5, pp. 2414–2421.

[8] J. C. Curlander, C. Wu, and A. Pang, "Automated preprocessing of spaceborne SAR data", Proc. IGARSS'82, pp. FA–1/3.11–6, June 1982.

[9] F.-K. Li, D. N. Held, J. C. Curlander, and C. Wu, "Doppler parameter estimation for spaceborne synthetic aperture radar", IEEE Trans. on Geoscience and Remote Sensing, vol. GE-23, no. 1, pp. 47–56, Jan 1985.

[10] J. Dall, "A fast autofocus algorithm for synthetic aperture radar processing", Proc. IEEE ICASSP, March, 1992, vol. 3, pp. III–5–III–8.

[11] J. Dall, "A new frequency domain autofocus algorithm for SAR", Proc. IGARSS '91, vol. 2, pp. 1069–1072, June 1991.

[12] P. Samczynski and K. Kulpa, "Coherent MapDrift technique", IEEE Trans. on Geoscience and Remote Sensing, vol. 48, no. 3, pp. 1505–1517, March 2010.

[13] T. M. Calloway and G. W. Donohoe, "Subaperture autofocus for synthetic aperture radar", Trans. Aerosp. Electron. Syst., vol. 30 no. 2, pp. 617–621, April 1994.

[14] H. M. J. Cantalloube and C. E. Nahum, "Motion compensation and autofocus of range/Doppler or two-dimensional processing for airborne synthetic aperture radar", Aerospace Science and Technology, vol. 2, issue 4, May 1998, pp. 251–263.

[15] H. M. J. Cantalloube and C. E. Nahum, "Multiscale local map-drift-driven multilateration SAR autofocus using fast polar format algorithm image synthesis", IEEE Trans. on Geoscience and Remote Sensing, vol. 49, no. 10, pp. 3730–3736, Oct 2010.

[16] J. R. Moreira, "A new method of aircraft motion error extraction from radar raw data for real time motion compensation", IEEE Trans. on Geoscience and Remote Sensing, vol. 28, no. 8, pp. 620–626, July 1990.

[17] J. R. Moreira, "Estimating the residual error of the reflectivity displacement method for aircraft motion error extraction from SAR raw data", Proc. IEEE Intern. Radar Conf., pp. 70–75, May 1990.

[18] S. Buckreuss, "Motion compensation for airborne SAR based on inertial data, RDM and GPS", IGARSS'94, vol. 4, pp. 1971–1973.

[19] D. M. Vavriv at al., "SAR Systems for Light-Weight Aircrafts", Proc. 2011 Microwaves, Radar and Remote Sensing Symp. MRRS 2011 (Kiev, Ukraine), pp. 15–19, 2011.

[20] O. O. Bezvesilniy, V. V. Vinogradov, and D. M. Vavriv, "Estimating Doppler centroid and autofocusing for airborne SAR", Proc. Int. Radar Symp. IRS 2005 (Berlin, Germany), pp. 59–63, 2005.